THE JOURNAL OF PHYSICAL CHEMISTRY Letters

Letter

Cite This: J. Phys. Chem. Lett. 2019, 10, 2657−2662

pubs.acs.org/JPCL

Regioselective Ultrafast Photoinduced Electron Transfer from Naphthols to Halocarbon Solvents

Subhajyoti Chaudhuri,[†] Atanu Acharya,[†,§] Erik T. J. Nibbering,[‡] and Victor S. Batista*[,†]

[†]Department of Chemistry, Yale University, P.O. Box 208107, New Haven, Connecticut 06520, United States

[‡]Max Born Institut für Nichtlineare Optik and Kurzzeitspektroskopie, Max Born Strasse 2A, 12489 Berlin, Germany

Supporting Information

ABSTRACT: Excited state decay of 2-naphthol (2N) in halocarbon solvents has been observed to be significantly slower when compared to that of 1-naphthol (1N). In this study, we provide new physical insights behind this observation by exploring the regioselective electron transfer (ET) mechanism from photoexcited 1N and 2N to halocarbon solvents at a detailed molecular level. Using state-of-the-art electronic structure calculations, we explore several configurations of naphthol−chloroform complexes and find that the proximity of the electron-accepting chloroform molecule to the electron-rich −OH group of the naphthol is the dominant factor affecting electron transfer rates. The origin of significantly slower electron transfer rates for 2N is traced back to the notably smaller electronic coupling when the electron-accepting chloroform molecule is on top of the aromatic ring distal to the −OH group. Our findings suggest that regioselective photoinduced electron transfer could thus be exploited to control electron transfer in substituted acenes tailored for specific applications.

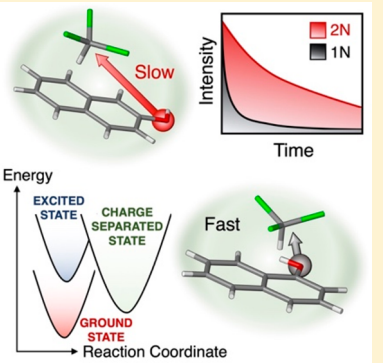

Photoinduced electron transfer plays a key role in light-harvesting molecular systems responsible for converting electromagnetic radiation into charge carriers.[1−6] Excited state processes are limited by the excited state lifetimes. The radiative decay pathway competes with the nonradiative pathways and typically involves charge separation and/or chemical changes. Understanding the molecular mechanisms of excited state decay is thus essential for a wide range of applications. One of the most important decay processes is via intermolecular electron transfer (ET), which is the focus of this Letter.

Significant efforts have been undertaken to elucidate ET processes by tuning the donor−acceptor interactions through variation of molecular structures[7] or by control of ET rates through molecular design of donor−acceptor dyad systems.[8−10] Time-resolved spectroscopic studies have revealed the relevant ET time scales as well as geometric aspects that control the relaxation mechanisms by regulating the arrangement and separation of specific donor and acceptor units.[11] The interplay between fast "on-contact" ET reaction dynamics and slow diffusional dynamics often makes it difficult to interpret solution-phase ET between freely moving donor and acceptor systems, and further intricacies occur upon the involvement of excited radical ion states.[12] Molecular design of donor−acceptor dyads with fixed donor−acceptor distances has enabled the analysis of ET rates as a function of free energy changes for a series of electron-acceptor moieties, eliminating the ambiguity that would otherwise be introduced with variable electron donor−acceptor distances.[13−15] However, photoinduced ET from solute to solvent is more difficult to characterize because of the bulk nature of the solvent.[16,17] Many solute−solvent conformations are conducive to faster ET, whereas other configurations would be ineffective. Nevertheless, conformations leading to fast ET often make photoinduced ET the most effective decay pathway. In fact, ET is often dominated by close contact interactions with the fluctuating first coordination shell of solvent, generating a distribution of solute−solvent configurations without significant diffusional character of donor−acceptor partners. This aspect has been understood to play a crucial role in donor−acceptor systems where the aromatic nature of both the donor and acceptor makes the $\pi-\pi$ orbital interactions the dominating factor. Examples for these can be found in important time-resolved ET studies using *N*,*N*-dimethylaniline as an electron-donating solvent and a variety of aromatic electron acceptors.[18−23] The size of such molecular systems makes computations prohibitively expensive with a state-of-the-art quantum chemical calculational methodology. Hence, we first study a significantly more compact halocarbon solvent as an electron-accepting case, with a moderately sized naphthol as the electron donor. With this, we analyze thermally accessible configurations to identify dominant configurations for efficient ET.

Previous studies have ascribed ET from electronically excited naphthol to the nonpolar carbon tetrachloride (CCl_4) solvent as the main mechanism for ultrafast fluorescence decay, as observed by time-correlated single-photon counting (TCSPC) experiments.[24,25] However, a

Received: February 12, 2019
Accepted: May 3, 2019
Published: May 3, 2019

DOI: 10.1021/acs.jpclett.9b00410
J. Phys. Chem. Lett. 2019, 10, 2657−2662

mechanism that could explain the appreciably slower excited state decay of 2-naphthol (2N) compared to that of 1-naphthol (1N) remains unknown and is the subject of this paper.

Here, we find new physical evidence for photoinduced ET-mediated decay of the naphthol excited state making the photoinduced ET from 1N much faster than that from 2N. We focus on studying ET to the solvent by explicitly modeling the electron-accepting solvent in complexation with the solute. We explore a distribution of configurations for the naphthol chromophore in close contact with the electron acceptor solvent in the first coordination sphere while modeling the rest of the surrounding solvent as a polarizable continuum dielectric.

We focus on chloroform because it is a solvent probe with directional character that allows for systematic exploration of interactions in the electron donor−acceptor complex. Polar solvents like water were ruled out because they would lead to chemical changes resulting from the photoacidic property of naphthols, thus defeating the purpose of studying photo-induced ET. A previous ET-mediated fluorescence quenching study was focused on CCl_4, a solvent without significant directionality.[24] The CCl_4 molecule interacts with the aromatic ring of naphthols, with the three C−Cl bonds forming an umbrella-like arrangement facing the naphthol fluorophore (Figure 1b).

Remarkably, the electronic excited state decay times differ by an order of magnitude when comparing 1N and 2N (1.4 ps in 1N vs 13 ps in 2N, as measured by UV/IR pump−probe spectroscopy) in CCl_4. The difference is even more significant in chloroform (70 ps in 1N vs 900 ps−1.9 ns in 2N), with 2N again exhibiting the slower decay (Figure 1a). Chloroform ($CHCl_3$) in the first solvation shell has the C−H bond usually pointing toward the naphthol (Figure 1c), thus functioning as a directional probe.

The analysis of energetically accessible configurations of naphthol−$CHCl_3$ complexes reveals the proximity of the electron-accepting solvent molecule to the proximal aromatic ring ($R^{(1)}$) as the primary factor governing the ET rates. The close contact arrangement provides understanding of configurations that dominate photoinduced ET in naphthols, providing a design principle for modulation of ET with −OH-substituted polyacene electron donors.

The configurations of 1N and 2N in contact with $CHCl_3$ were obtained in a continuum dielectric environment, as described by the CPCM[26] model in Q-Chem 5.0.[27] The $CHCl_3$ electron acceptor was found to settle on top of the naphthol (Figure 2d) with the C−H bond pointing toward one of the rings ($R^{(1)}$ or $R^{(2)}$), as described by the ground electronic state at the B3LYP[28]-D (empirical dispersion correction from Chai & Head-Gordon[29])/6-31+G(d,p) level of theory.

In nonpolar or weakly polar solvents, the ^1L_a state is higher than the ^1L_b state. Thus, following Kasha's rule, only the ^1L_b state emission is observed because fluorescence emission is observed from the lowest-lying excited state, S_1.[30−34] The more ionic ^1L_a state[25,35−37] is formed predominantly by a LUMO ← HOMO transition, whereas the ^1L_b state is primarily a combination of LUMO ← HOMO − 1 and LUMO + 1 ← HOMO.[38] TDDFT was used to generate the excited state configurations at the B3LYP-D/6-31+G(d,p) level of theory. However, TDDFT was found to severely underestimate the ^1L_a energy and erroneously label it as the lowest excited state,[39] leading to drastic errors in prediction of the emission and absorption spectra for naphthols. To circumvent this problem, all excitation energies were computed at the EOM-CCSD[40−48]/6-31+G(d,p) level of theory as implemented in Q-Chem 5.0. EOM-CCSD allows us to identify the fluorescent ^1L_b state correctly and obtain all relative energies consistently for the various isomers of naphthols.

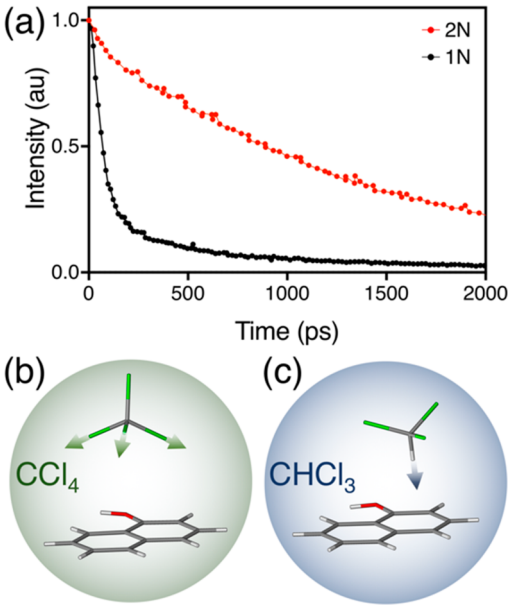

Figure 1. (a) TCSPC measurements of 1N and 2N in $CHCl_3$. (b) Optimized ground state geometry of 1N in CCl_4 showing C−Cl bonds forming an umbrella-like configuration on the naphthol. (c) $CHCl_3$ with the C−H bond pointing toward the naphthol aromatic ring.

Constrained-DFT (CDFT) optimizations provided the charge-separated (CS) state, as generated by photoinduced ET, with the hole (i.e., missing electron) constrained on the naphthol (donor) and the electron on the $CHCl_3$ (acceptor) molecule (Figure 3). Preliminary CDFT calculations (see the SI) show that $CHCl_3^-$ dissociates into $CHCl_2$ and Cl^-, consistent with earlier studies.[49,50] Because the dissociation succeeds the ET, it is not relevant for this study of ultrafast dynamics of photoinduced ET. Therefore, we analyze the CS state with constraints on the C−Cl and C−H bond lengths derived from a separate optimization of $CHCl_3^-$ at the MP2/6-311++G(d,p) level of theory. This allows us to model the acceptor moiety after ET, but before dissociation. We find that in the CS state $CHCl_3^-$ is placed above the naphthol ring with the C−H bond pointing toward one of the carbons of the naphthol. To gain further insights into stable CS state configurations, we performed optimizations with geometry constraints and obtained a distribution of configurations with the C−H bond of chloroform pointing toward each of the carbons of naphthol. Due to negligible Boltzmann weights, the higher-energy configurations were considered statistically insignificant, and only the energetically favorable configurations were considered for this study (Figure 2c). The more favored conformations correspond to the C−H bond pointing toward $C^{(2)}$ and $C^{(4)}$ of 1N and $C^{(1)}$ of 2N (Figure 2d). Those configurations correspond to resonance structures (see the SI) stabilized by $C^{(2)}$ and $C^{(4)}$ that are the electron-rich centers of 1N and 2N.

ET rates were computed, according to Marcus theory, using the computed parameters for the reorganization energy,

DOI: 10.1021/acs.jpclett.9b00410
J. Phys. Chem. Lett. 2019, 10, 2657−2662

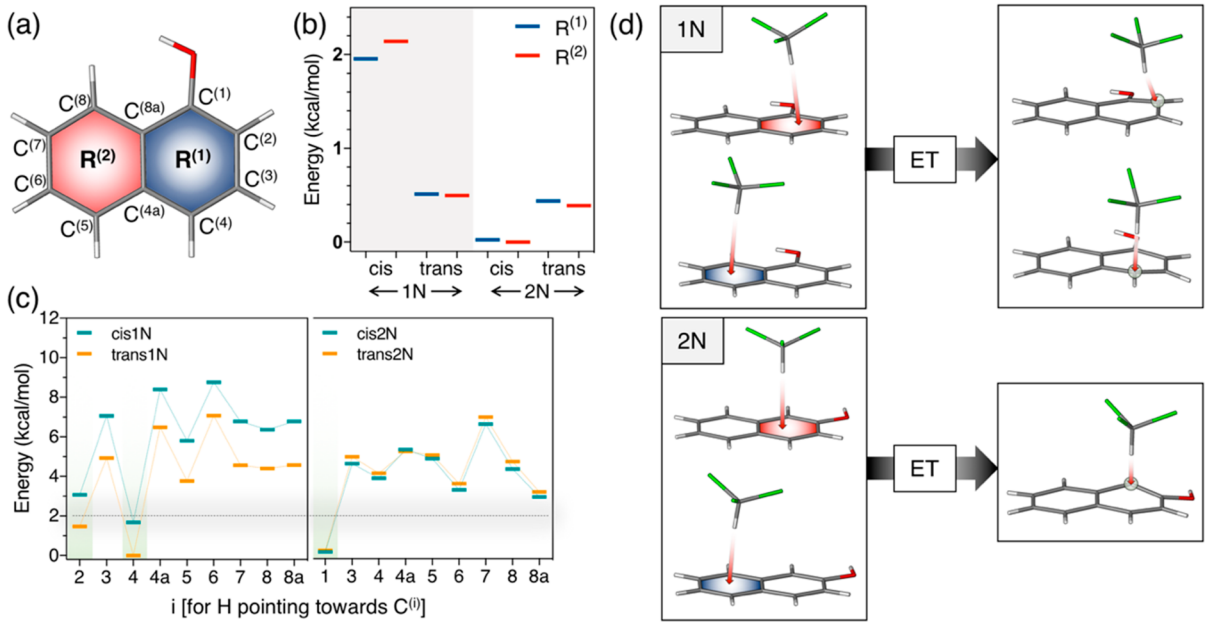

Figure 2. (a) Labeling of the aromatic rings of 1N. Energies of the 1N/2N−$CHCl_3$ complex for various configurations in the (b) ground state and (c) charge-separated state. (d) Representative low-energy configurations for *cis*-1N and *cis*-2N before and after ET. Red arrows show the C−H bond pointing (left) toward the center of the ring (in the ground state) or (right) to a carbon atom (in the charge-separated state).

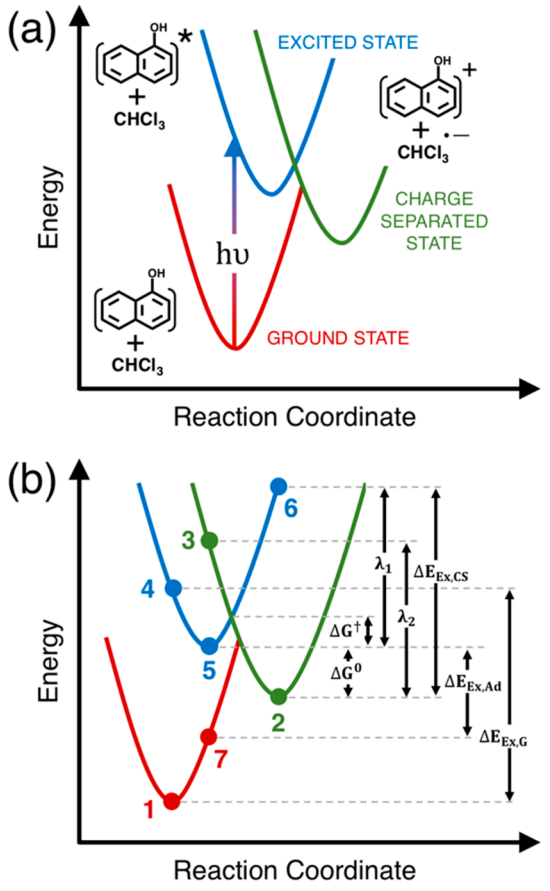

Figure 3. Schematic diagram showing the ground (red), excited (blue), and CS (green) energy surfaces, including (a) formal oxidation states and (b) Marcus parameters required to compute photoinduced ET rates.

electronic coupling, and free energy. Therefore, reactants and products are described by harmonic states (Figure 3a) at the semiclassical level.[51−53] For weakly coupled donor−acceptor systems, the ET rates (k_{ET}) depend on (i) the free energy of reaction (ΔG^0), (ii) the reorganization energy (λ), and (iii) the electronic coupling (H_{if}), as follows

$$k_{ET} = \frac{2\pi |H_{if}|^2}{\hbar\sqrt{4\pi\lambda k_B T}} \exp\left(-\frac{(\Delta G^0 + \lambda)^2}{4\lambda k_B T}\right) \quad (1)$$

Therefore, the ET times (t_{comp}) can be readily obtained as follows

$$t_{comp} = \frac{1}{k_{ET}} \quad (2)$$

The free energy values (ΔG^0) are calculated as the free energy differences between the CS and excited states (Figure 3b)

$$\Delta G^0 = E_2 - E_5 \quad (3)$$

The reorganization energy (λ) is computed as a geometric average of the ground and CS state reorganization energies λ_1 and λ_2 (see Figure 3b), obtained as follows

$$\lambda_1 = E_3 - E_2 \quad (4)$$

$$\lambda_2 = E_6 - E_5 \quad (5)$$

Under the displaced harmonic oscillator approximation,[54] $\lambda_1 = \lambda_2$. However, the two reorganization energies are usually slightly different;[55] therefore, the effective reorganization energy (λ) is computed as follows[55]

$$\lambda = \frac{\lambda_1 + \lambda_2}{2} \quad (6)$$

The activation free energy ($\Delta G^\dagger$) is defined by ΔG^0 and λ as follows

$$\Delta G^\dagger = \frac{(\Delta G^0 + \lambda)^2}{4\lambda} \quad (7)$$

DOI: 10.1021/acs.jpclett.9b00410
J. Phys. Chem. Lett. 2019, 10, 2657−2662

Table 1. ET Times and Marcus Parameters

H pointing to								
ground state	CS state	isomer	ΔG^0 (eV)	λ (eV)	H_{if} (eV)	$\Delta G^{\dagger}$ (eV)	t_{comp} (ps)	t_{TCSPC} (ps)
$R^{(1)}$	$C^{(2)}$	*cis*-1N	−0.41	1.35	0.01	0.16	269	70 (0.92)
		trans-1N	−0.45	1.37	0.02	0.15	85	1.5×10^3 (0.08)
	$C^{(4)}$	*cis*-1N	−0.48	1.25	0.01	0.12	51	
		trans-1N	−0.51	1.27	0.02	0.11	16	
$R^{(2)}$	$C^{(2)}$	*cis*-1N	−0.42	1.34	0.02	0.16	63	
		trans-1N	−0.45	1.34	0.02	0.15	53	
	$C^{(4)}$	*cis*-1N	−0.48	1.37	0.02	0.15	39	
		trans-1N	−0.51	1.36	0.02	0.13	29	
$R^{(1)}$	$C^{(1)}$	*cis*-2N	−0.31	1.42	0.02	0.16	64	<40 (0.2)
		trans-2N	−0.29	1.40	0.02	0.16	94	900 (0.4)
$R^{(2)}$		*cis*-2N	−0.47	1.42	0.002	0.16	15×10^3	1.9×10^3 (0.4)
		trans-2N	−0.46	1.39	0.001	0.16	55×10^3	

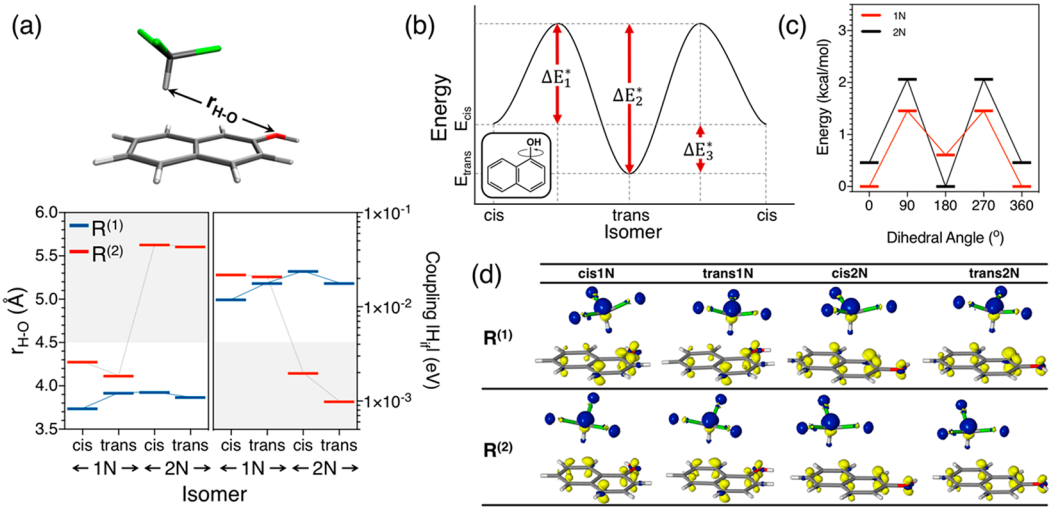

Figure 4. (a) Distances between H of $CHCl_3$ and O of naphthol for different configuration with the solvent on top of $R^{(1)}$ and $R^{(2)}$ and corresponding electronic couplings. (b) Schematic diagram of a dihedral scan and relevant energies. (c) Dihedral scans of $C^{(8a)}$–$C^{(1)}$–O–H (for 1N) and $C^{(1)}$–$C^{(2)}$–O–H (for 2N) in the excited state. (d) Change of electron density before and after ET (density goes from yellow to blue during ET).

Table 2. Excited-State Isomerization Times and Boltzmann Populations

molecule	isomer	isomerization time (ps)	population (%)
1N	cis	3	76
	trans	1	24
2N	cis	4	52
	trans	8	48

The electronic couplings (H_{if}) are computed with the fragment-charge difference (FCD) method[56] under the two-state approximation (i.e., assuming that the reactant and product diabatic states are linear combinations of the eigenstates). The naphthol and $CHCl_3$ molecules are defined as the donor and acceptor fragments, respectively. The states are chosen according to the maximum charge differences between the two fragments, as implemented in Q-Chem 5.0 at the DFT ωB97x-D/6-31+G(d,p) level of theory.

Table 1 lists the calculated Marcus parameters and ET rates. The ET from 1N is significantly faster (t_{comp} = 16–269 ps) than that from 2N (ns), consistent with TCSPC experiments. In fact, multiexponential fitting of the decay curves shows that the major decay time for 1N is <100 ps, while that for 2N is 1.9 ns.

Isomerization times of <10 ps were obtained, according to transition state theory (see Table 2 and Figure 4a,b), at the EOM-CCSD/6-31+G(d,p) level using Q-Chem 5.0, with excited state barriers obtained by scanning the $C^{(8a)}$–$C^{(1)}$–O–H (1N) and $C^{(1)}$–$C^{(2)}$–O–H (2N) dihedral angles.

Ultrafast isomerization leads to faster ET routes, with isomerization preceding ET. However, we observe a significantly slow component of ET and fluorescence quenching in 2N due to the noticeably slow ET in both *cis*- and *trans*-2N (with $CHCl_3$ pointing toward $R^{(2)}$ and nearly identical Boltzmann populations of both isomers in the excited state).

$$k_{cis\rightarrow trans} = \frac{k_B T}{\hbar} \exp\left(-\frac{\Delta E_1^*}{k_B T}\right) \quad (8)$$

$$k_{trans\rightarrow cis} = \frac{k_B T}{\hbar} \exp\left(-\frac{\Delta E_2^*}{k_B T}\right) \quad (9)$$

DOI: 10.1021/acs.jpclett.9b00410
J. Phys. Chem. Lett. 2019, 10, 2657–2662

$$\frac{N_{cis}}{N_{trans}} = \frac{k_B T}{\hbar} \exp\left(-\frac{\Delta E_3^*}{k_B T}\right) \quad (10)$$

As noted from Table 1, configurations with low ΔG^0 also have low λ, resulting in similar $\Delta G^\dagger$ for all cases. Electronic couplings are thus important factors that modulate ET rates.

The plot of electron densities differences, before and after ET (Figure 4d), shows that the electron density is transferred from the oxygen of the naphthol to the $CHCl_3$ molecule. Being on top of $R^{(1)}$ allows the solvent molecule to accept the electron much faster. However, when the electron-accepting solvent molecule is on top of $R^{(2)}$, especially for 2N, ET is slower because the separation between the electron-rich oxygen and the $CHCl_3$ is larger and thus the electronic coupling is significantly smaller (Figure 4c).

In summary, quantum chemical calculations on several statistically relevant configurations allowed us to elucidate the origin of significantly different fluorescence lifetimes of photoexcited naphthols in halogenated solvents. The observed differences in ET dynamics stem from the differences in electronic couplings when comparing 1N and 2N. Differences in reorganization energies are nearly compensated by concomitant differences in ET free energies. The differences in couplings are controlled by different electron donor−acceptor distances, as determined by the closer contact of the −OH group with $CHCl_3$ in 1N compared to that in 2N, thereby rationalizing the significantly different fluorescence quenching lifetimes observed in experiments.

Our findings suggest that increasing the number of fused aromatic rings in the chromophore can allow us to gain control over fluorescence quenching times through modulation of the separation between the electron-accepting solvent molecules in the first coordination sphere and the electron-rich center of the −OH-substituted acenes. The regioselective ET discussed in this study can be utilized for several practical applications, an evident one being the design of photoswitching molecular probes.

■ ASSOCIATED CONTENT

Supporting Information

The Supporting Information is available free of charge on the ACS Publications website at DOI: 10.1021/acs.jpclett.9b00410.

Computational method, information about calculations performed, necessity of using EOM-CCSD for excited states, comparison of free and reorganization energies with and without explicit solvent, and coordinates of optimized structures (PDF)

■ AUTHOR INFORMATION

Corresponding Author

*E-mail: victor.batista@yale.edu.

ORCID

Subhajyoti Chaudhuri: 0000-0001-8297-1123
Atanu Acharya: 0000-0002-6960-7789
Erik T. J. Nibbering: 0000-0001-5874-8052
Victor S. Batista: 0000-0002-3262-1237

Present Address

§(A.A.) School of Physics, Georgia Institute of Technology, Atlanta, Georgia 30332, United States.

Notes

The authors declare no competing financial interest.

■ ACKNOWLEDGMENTS

V.S.B. acknowledges support by the AFOSR Grant #FA9550-17-0198 and high-performance computing time from NERSC. This work used the Extreme Science and Engineering Discovery Environment (XSEDE), which is supported by National Science Foundation Grant Number ACI-1053575. A.A. acknowledges supercomputer time from the Extreme Science and Engineering Discovery Environment (XSEDE) under Grant TG-CHE170024. E.T.J.N. acknowledges support from the German Science Foundation (Project Number DFG-NI 492/11-1).

■ REFERENCES

(1) Grätzel, M. Solar Energy Conversion by Dye-Sensitized Photovoltaic Cells. *Inorg. Chem.* **2005**, *44* (20), 6841−6851.
(2) Gust, D.; Moore, T. A.; Moore, A. L. Solar Fuels via Artificial Photosynthesis. *Acc. Chem. Res.* **2009**, *42* (12), 1890−1898.
(3) Polívka, T.; Sundström, V. Ultrafast Dynamics of Carotenoid Excited States-From Solution to Natural and Artificial Systems. *Chem. Rev.* **2004**, *104* (4), 2021−2072.
(4) Bottari, G.; De La Torre, G.; Guldi, D. M.; Torres, T. Covalent and Noncovalent Phthalocyanine-Carbon Nanostructure Systems: Synthesis, Photoinduced Electron Transfer, and Application to Molecular Photovoltaics. *Chem. Rev.* **2010**, *110* (11), 6768−6816.
(5) Nelson, N.; Yocum, C. F. Structure and Function of Photosystems I and II. *Annu. Rev. Plant Biol.* **2006**, *57* (1), 521−565.
(6) Bixon, M.; Jortner, J. Electron Transfer—from Isolated Molecules to Biomolecules. *Adv. Chem. Phys.* **2007**, *106*, 35−202.
(7) Pellegrin, Y.; Odobel, F. Molecular Devices Featuring Sequential Photoinduced Charge Separations for the Storage of Multiple Redox Equivalents. *Coord. Chem. Rev.* **2011**, *255* (21−22), 2578−2593.
(8) Gilat, S. L.; Kawai, S. H.; Lehn, J.-M. Light-Triggered Molecular Devices: Photochemical Switching of Optical and Electrochemical Properties in Molecular Wire Type Diarylethene Species. *Chem. Eur. J.* **1995**, *1* (5), 275−284.
(9) Holten, D.; Bocian, D. F.; Lindsey, J. S. Probing Electronic Communication in Covalently Linked Multiporphyrin Arrays. A Guide to the Rational Design of Molecular Photonic Devices. *Acc. Chem. Res.* **2002**, *35* (1), 57−69.
(10) Meier, H. Conjugated Oligomers with Terminal Donor−Acceptor Substitution. *Angew. Chem. Int. Ed.* **2005**, *44* (17), 2482−2506.
(11) Kumpulainen, T.; Lang, B.; Rosspeintner, A.; Vauthey, E. Ultrafast Elementary Photochemical Processes of Organic Molecules in Liquid Solution. *Chem. Rev.* **2017**, *117* (16), 10826−10939.
(12) Koch, M.; Rosspeintner, A.; Adamczyk, K.; Lang, B.; Dreyer, J.; Nibbering, E. T. J.; Vauthey, E. Real-Time Observation of the Formation of Excited Radical Ions in Bimolecular Photoinduced Charge Separation: Absence of the Marcus Inverted Region Explained. *J. Am. Chem. Soc.* **2013**, *135* (26), 9843−9848.
(13) Dance, Z. E. X.; Ahrens, M. J.; Vega, A. M.; Ricks, A. B.; McCamant, D. W.; Ratner, M. A.; Wasielewski, M. R. Direct Observation of the Preference of Hole Transfer over Electron Transfer for Radical Ion Pair Recombination in Donor-Bridge-Acceptor Molecules. *J. Am. Chem. Soc.* **2008**, *130* (3), 830−832.
(14) Closs, G. L.; Miller, J. R. Intramolecular Long-Distance Electron Transfer in Organic Molecules. *Science* **1988**, *240* (4851), 440−447.
(15) Miller, J. R.; Calcaterra, L. T.; Closs, G. L. Intramolecular Long-Distance Electron Transfer in Radical Anions. The Effects of Free Energy and Solvent on the Reaction Rates. *J. Am. Chem. Soc.* **1984**, *106* (10), 3047−3049.
(16) Shirota, H.; Pal, H.; Tominaga, K.; Yoshihara, K. Substituent Effect and Deuterium Isotope Effect of Ultrafast Intermolecular

DOI: 10.1021/acs.jpclett.9b00410
J. Phys. Chem. Lett. 2019, 10, 2657−2662

Electron Transfer: Coumarin in Electron-Donating Solvent. *J. Phys. Chem. A* **1998**, *102* (18), 3089−3102.
(17) Ghosh, H. N.; Verma, S.; Nibbering, E. T. J. Ultrafast Forward and Backward Electron Transfer Dynamics of Coumarin 337 in Hydrogen-Bonded Anilines As Studied with Femtosecond UV-Pump/IR-Probe Spectroscopy. *J. Phys. Chem. A* **2011**, *115* (5), 664−670.
(18) Castner, E. W.; Kennedy, D.; Cave, R. J. Solvent as Electron Donor: Donor/Acceptor Electronic Coupling Is a Dynamical Variable. *J. Phys. Chem. A* **2000**, *104* (13), 2869−2885.
(19) Scherer, P. O. J.; Tachiya, M. Computer Simulation Studies of Electron Transfer Parameters for Cyanoanthracene/N,N-Dimethylaniline Solutions. *J. Chem. Phys.* **2003**, *118* (9), 4149−4156.
(20) Morandeira, A.; Fürstenberg, A.; Gumy, J.-C.; Vauthey, E. Fluorescence Quenching in Electron-Donating Solvents. 1. Influence of the Solute-Solvent Interactions on the Dynamics. *J. Phys. Chem. A* **2003**, *107* (28), 5375−5383.
(21) Morandeira, A.; Fürstenberg, A.; Vauthey, E. Fluorescence Quenching in Electron-Donating Solvents. 2. Solvent Dependence and Product Dynamics. *J. Phys. Chem. A* **2004**, *108* (40), 8190−8200.
(22) Saik, V. O.; Goun, A. A.; Fayer, M. D. Photoinduced Electron Transfer and Geminate Recombination for Photoexcited Acceptors in a Pure Donor Solvent. *J. Chem. Phys.* **2004**, *120* (20), 9601−9611.
(23) Rosspeintner, A.; Angulo, G.; Vauthey, E. Driving Force Dependence of Charge Recombination in Reactive and Nonreactive Solvents. *J. Phys. Chem. A* **2012**, *116* (38), 9473−9483.
(24) Chaudhuri, S.; Rudshteyn, B.; Prémont-Schwarz, M.; Pines, D.; Pines, E.; Huppert, D.; Nibbering, E. T.; Batista, V. S. Ultrafast Photo-Induced Charge Transfer of 1-Naphthol and 2-Naphthol to Halocarbon Solvents. *Chem. Phys. Lett.* **2017**, *683*, 49−56.
(25) Messina, F.; Prémont-Schwarz, M.; Braem, O.; Xiao, D.; Batista, V. S.; Nibbering, E. T. J.; Chergui, M. Ultrafast Solvent-Assisted Electronic Level Crossing in 1-Naphthol. *Angew. Chem. Int. Ed.* **2013**, *52* (27), 6871−6875.
(26) Cossi, M.; Rega, N.; Scalmani, G.; Barone, V. Energies, Structures, and Electronic Properties of Molecules in Solution with the C-PCM Solvation Model. *J. Comput. Chem.* **2003**, *24* (6), 669−681.
(27) Shao, Y.; Gan, Z.; Epifanovsky, E.; Gilbert, A. T.; Wormit, M.; Kussmann, J.; Lange, A. W.; Behn, A.; Deng, J.; Feng, X.; et al. Advances in Molecular Quantum Chemistry Contained in the Q-Chem 4 Program Package. *Mol. Phys.* **2015**, *113* (2), 184−215.
(28) Becke, A. D. Density-functional Thermochemistry. III. The Role of Exact Exchange. *J. Chem. Phys.* **1993**, *98* (7), 5648−5652.
(29) Chai, J.-D.; Head-Gordon, M. Long-Range Corrected Hybrid Density Functionals with Damped Atom−Atom Dispersion Corrections. *Phys. Chem. Chem. Phys.* **2008**, *10* (44), 6615−6620.
(30) Suzuki, S.; Baba, H. Polarization Study of the Fluorescent State of the Hydrogen Bonded α-Naphthol. *Bull. Chem. Soc. Jpn.* **1967**, *40* (9), 2199−2200.
(31) Magnes, B.-Z.; Strashnikova, N. V.; Pines, E. Evidence for ^1L_a, ^1L_b Dual State Emission in 1-Naphthol and 1-Methoxynaphthalene Fluorescence in Liquid Solutions. *Isr. J. Chem.* **1999**, *39* (3−4), 361−373.
(32) Knochenmuss, R.; Muiño, P. L.; Wickleder, C. Vibronic Coupling and Microscopic Solvation of 1-Naphthol. *J. Phys. Chem.* **1996**, *100* (27), 11218−11227.
(33) Suzuki, S.; Fujii, T.; Imai, A.; Akahori, H. The Fluorescent Level Inversion of Dual Fluorescences and the Motional Relaxation of Excited State Molecules in Solutions. *J. Phys. Chem.* **1977**, *81* (16), 1592−1598.
(34) Suzuki, S.; Fujii, T.; Sato, K. The Temperature Dependence of the Fluorescence and Polarization Spectra of 1-Naphthol. *Bull. Chem. Soc. Jpn.* **1972**, *45* (6), 1937−1938.
(35) Grimme, S.; Parac, M. Substantial Errors from Time-Dependent Density Functional Theory for the Calculation of Excited States of Large π Systems. *ChemPhysChem* **2003**, *4* (3), 292−295.
(36) Richard, R. M.; Herbert, J. M. Time-Dependent Density-Functional Description of the ^1L_a State in Polycyclic Aromatic Hydrocarbons: Charge-Transfer Character in Disguise? *J. Chem. Theory Comput.* **2011**, *7* (5), 1296−1306.
(37) Wong, B. M.; Hsieh, T. H. Optoelectronic and Excitonic Properties of Oligoacenes: Substantial Improvements from Range-Separated Time-Dependent Density Functional Theory. *J. Chem. Theory Comput.* **2010**, *6* (12), 3704−3712.
(38) Xiao, D.; Prémont-Schwarz, M.; Nibbering, E. T. J.; Batista, V. S. Ultrafast Vibrational Frequency Shifts Induced by Electronic Excitations: Naphthols in Low Dielectric Media. *J. Phys. Chem. A* **2012**, *116* (11), 2775−2790.
(39) Acharya, A.; Chaudhuri, S.; Batista, V. S. Can TDDFT Describe Excited Electronic States of Naphthol Photoacids? A Closer Look with EOM-CCSD. *J. Chem. Theory Comput.* **2018**, *14* (2), 867−876.
(40) Rowe, D. Equations-of-Motion Method and the Extended Shell Model. *Rev. Mod. Phys.* **1968**, *40* (1), 153.
(41) Emrich, K. An Extension of the Coupled Cluster Formalism to Excited States:(II). Approximations and Tests. *Nucl. Phys. A* **1981**, *351* (3), 397−438.
(42) Geertsen, J.; Rittby, M.; Bartlett, R. J. The Equation-of-Motion Coupled-Cluster Method: Excitation Energies of Be and CO. *Chem. Phys. Lett.* **1989**, *164* (1), 57−62.
(43) Stanton, J. F.; Bartlett, R. J. The Equation of Motion Coupled-Cluster Method. A Systematic Biorthogonal Approach to Molecular Excitation Energies, Transition Probabilities, and Excited State Properties. *J. Chem. Phys.* **1993**, *98* (9), 7029−7039.
(44) Krylov, A. I. Equation-of-Motion Coupled-Cluster Methods for Open-Shell and Electronically Excited Species: The Hitchhiker's Guide to Fock Space. *Annu. Rev. Phys. Chem.* **2008**, *59*, 433−462.
(45) Stanton, J. F.; Gauss, J. A Discussion of Some Problems Associated with the Quantum Mechanical Treatment of Open-Shell Molecules. *Adv. Chem. Phys.* **2003**, *125*, 101−146.
(46) Comeau, D. C.; Bartlett, R. J. The Equation-of-Motion Coupled-Cluster Method. Applications to Open-and Closed-Shell Reference States. *Chem. Phys. Lett.* **1993**, *207* (4−6), 414−423.
(47) Stolarczyk, L. Z.; Monkhorst, H. J. Coupled-Cluster Method with Optimized Reference State. *Int. J. Quantum Chem.* **1984**, *26* (S18), 267−291.
(48) Sinha, D.; Mukhopadhyay, S.; Mukherjee, D. A Note on the Direct Calculation of Excitation Energies by Quasi-Degenerate MBPT and Coupled-Cluster Theory. *Chem. Phys. Lett.* **1986**, *129* (4), 369−374.
(49) Staneke, P. O.; Groothuis, G.; Ingemann, S.; Nibbering, N. M. M. Formation, Stability and Structure of Radical Anions of Chloroform, Tetrachloromethane and Fluorotrichloromethane in the Gas Phase. *Int. J. Mass Spectrom. Ion Processes* **1995**, *142* (1−2), 83−93.
(50) Isse, A. A.; Lin, C. Y.; Coote, M. L.; Gennaro, A. Estimation of Standard Reduction Potentials of Halogen Atoms and Alkyl Halides. *J. Phys. Chem. B* **2011**, *115* (4), 678−684.
(51) Marcus, R. A. Electron Transfer Reactions in Chemistry. Theory and Experiment. *Rev. Mod. Phys.* **1993**, *65* (3), 599−610.
(52) Marcus, R. A. On the Theory of Oxidation-Reduction Reactions Involving Electron Transfer. I. *J. Chem. Phys.* **1956**, *24* (5), 966−978.
(53) Chaudhuri, S.; Hedström, S.; Méndez-Hernández, D. D.; Hendrickson, H. P.; Jung, K. A.; Ho, J.; Batista, V. S. Electron Transfer Assisted by Vibronic Coupling from Multiple Modes. *J. Chem. Theory Comput.* **2017**, *13* (12), 6000−6009.
(54) Marcus, R. A.; Sutin, N. Electron Transfers in Chemistry and Biology. *Biochim. Biophys. Acta, Rev. Bioenerg.* **1985**, *811* (3), 265−322.
(55) Parson, W. W.; Chu, Z. T.; Warshel, A. Reorganization Energy of the Initial Electron-Transfer Step in Photosynthetic Bacterial Reaction Centers. *Biophys. J.* **1998**, *74* (1), 182−191.
(56) Voityuk, A. A.; Rösch, N. Fragment Charge Difference Method for Estimating Donor−Acceptor Electronic Coupling: Application to DNA π-Stacks. *J. Chem. Phys.* **2002**, *117* (12), 5607−5616.

DOI: 10.1021/acs.jpclett.9b00410
J. Phys. Chem. Lett. 2019, 10, 2657−2662